Effect of disorder potential on the dynamics of resonantly excited incoherent free exciton-polariton fluids in high-Q GaAs microcavities

A. A. Demenev,[1] S. N. Tereshko,[1] N. A. Gippius,[1,2] and V. D. Kulakovskii[1,3]
[1]*Osipyan Institute of Solid State Physics, Russian Academy of Science, Chernogolovka 142432, Russia*
[2]*Skolkovo Institute of Science and Technology, Bolshoy Boulevard 30, Building 1, Moscow 121205, Russia*
[3]*National Research University Higher School of Economics, Moscow 101000, Russia*

(Received 11 August 2023; revised 1 February 2024; accepted 5 February 2024; published 21 February 2024)

The temporal behavior of the lower polariton (LP) distribution in the reciprocal space, $n_{\mathrm{LP}}(k)$, and formation of long-range spatial coherence are investigated in a nonequilibrium incoherent LP fluid generated resonantly with picosecond optical pulses at 2 K in a high-Q planar GaAs/AlAs microcavity with 12 InGaAs quantum wells. The dynamics of $n_{\mathrm{LP}}(k)$ is found to be independent of excitation density and well described within the framework of linear Schrödinger equations taking into account random potential disorder, δE_{LP}, and finite lifetime of LPs, up to LP density $n_{\mathrm{LP}}(t=0) = 7 \times 10^{10}$ cm^{-2} (3.5 orders of magnitude greater than the threshold density of Bose-Einstein condensation for LPs). This is explained by the smallness of the ratios of LP interaction energy to both the mean kinetic energy and potential disorder. The contribution of interparticle interaction to the formation of spatial coherence in the LP fluid is insignificant at $E_{\mathrm{int}} \ll \delta E_{\mathrm{LP}}$, but becomes noticeable already at $E_{\mathrm{int}} \approx 0.2\delta E_{\mathrm{LP}}$, despite the fact that its effect on the k distribution of LPs remains insignificant. Coherence length L_c in LP fluid with $n_{\mathrm{LP}}(t=0) = 2$ and 7×10^{10} cm^{-2} in the region with $\delta E_{\mathrm{LP}} = 0.15$ meV at $t = 160$ ps increases to 4.1 and 5.3 μm, respectively, whereas in an incoherent Bose gas with the same $n_{\mathrm{LP}}(k)$ it is equal to 3.6 μm.

DOI: 10.1103/PhysRevB.109.085423

I. INTRODUCTION

The unique properties of semiconductor microcavities (MCs) offer a way for experimental observation of exciton-polariton condensate in a wide temperature range up to room temperature [1–16] which opens up enormous opportunities both for fundamental research in many-body physics and for technological applications. The polaritons formed during the light-exciton interaction in the regime of strong exciton-photon coupling are ultralight boson quasiparticles with effective mass $m_{\mathrm{LP}} < 10^{-4} m_e$. They exhibit coherent properties at relatively low densities of about 10^7 cm^{-2} at $T = 2$ K and 10^9 cm^{-2} at room temperatures [17]. The magnitude of their interparticle interaction can be easily controlled by changing detuning of the exciton and photon modes in the MC [18,19]. The presence of a photonic component makes it possible to use optical methods not only to form nonequilibrium polariton condensates with desired properties but also to control transitions between them on the micron and picosecond scales.

The unambiguous relationship between the wave vector and energy of the emitting polariton and the emitted light quantum allows us to measure the momentum and energy distributions of polaritons, and to get a complete picture of the dynamics of many-particle interactions using various optical methods. Flexible control of a polariton system enabled by the dual exciton-photon nature of polaritons holds much promise not only for fundamental research in many-body physics, but for their use in all-optical devices [20–24].

By now condensation of cavity exciton polaritons on the lower polariton (LP) branch has been extensively studied using resonant excitation of excitonlike LPs at large lateral wave vectors and interband excitation generating hot electrons and holes in quantum wells [1–8,10,17,25–29]. In these investigations the polariton condensate on the LP branch is formed within several tens of picoseconds after picosecond pumping with a density above the critical value. Relatively short times of condensate formation are achieved by bosonic stimulation of the exciton scattering from the excited dense long-lived exciton reservoir into the condensate state after reaching the quantum degeneracy of the LP states at the LP band bottom [30–33]. The LP spatial coherence was found to expand with a high velocity of $\approx 10^8$ cm/s [25,29]; however, the coherence length L_c in the investigated condensates does not exceed several tens of microns. The main reasons for condensate decoherence are the potential disorder and interaction with the exciton reservoir [34–36]. The disorder can lead to formation of a Bose-glass insulating phase in which LP condensates in different traps become phase locked [37–40].

Condensate decoherence was found to drastically decrease in the case of all-optical trapping of polaritons via shaping the nonresonant pump profile [11,16,41–44] or direct resonant coherent excitation of LPs with picosecond pump pulses at the normal to the MC plane, when the exciton reservoir remains empty [45,46]. In the last case the first-order spatial correlation function $g^{(1)}(\mathbf{r}_1, \mathbf{r}_2)$ [47,48] in the excited condensate is nearly independent of the excitation density and remains high until the polariton blueshift gets comparable to the characteristic amplitude of the disorder potential δE_{LP}. The disorder causes short-range phase fluctuations as well as vortex formation but still has little effect on the overall coherence.

In the absence of an exciton reservoir, the energy relaxation time of nonequilibrium free LPs increases strongly; there-

fore, studies of LP condensation in a pure polariton fluid became possible only after the advent of high-Q MCs which ensured LP lifetime of $\tau_{\rm LP} > 100$ ps. The first experiments of optical trapping of polaritons were carried out with LPs in exciton-free annular optical traps realized using nonresonant excitation of a dense excitonic reservoir in a ring of about 20 μm in diameter [41,42]. The reservoir creates a two-dimensional (2D) repulsive potential necessary to confine escaping LPs inside the ring of 10 μm. The decreased interaction of LPs with excitons was found to lead to a pronounced narrowing of the condensate emission line [41]. Sun *et al.* [42] reported that $\tau_{\rm LP} = 270$ ps is sufficient for LP thermalization in such a trap at $T = 20$ K in the case of continuous excitation below the LP condensation threshold. However, it should be noted that the de Broglie wavelength of LPs with energy $E_{\rm kin} \approx 1$ meV localized in the trap of 10 μm is comparable to its diameter. Therefore, their properties are strongly affected by the interaction with the exciton reservoir in the photoexcited ring [49–52] and, in addition, by their localization.

In this paper, we study time evolution of a nonequilibrium incoherent *really* free polariton fluid excited resonantly in a planar GaAs/AlAs MC with a relatively small LP disorder potential $\delta E_{\rm LP} = 100$–300 μeV in the absence of both an exciton reservoir and potential barriers. The fluid with densities of LPs up to $n_{\rm LP} \approx 10^{11}$ cm^{-2}, which is much higher than the critical value for their condensation, was resonantly excited in a spot with a diameter of 100 μm in a wide range of wave vectors $2|\mathbf{k}| \lesssim 2.5$ μm^{-1} using incoherent converging picosecond optical pulses at $T = 2$ K. The lifetime of LPs in the investigated MC $\tau_{\rm LP} \approx 170$ ps made it possible to study their dynamics in real and reciprocal spaces within 1.5 ns.

The temporal evolution of the momentum distribution of LPs, $n_{\rm LP}(k)$, in an excited spot was found to be completely determined by elastic scattering on the disorder potential. At the initial stage the runaway of high-energy LPs outside the excited region leads to a rapid decrease in the average kinetic energy $\langle E_{\rm kin}\rangle$ of LPs remaining in the excited spot. This stage is over in about 100 ps when the LP fluid expands to dimensions of the order of the LP mean free path. After that, not only the average energy of LPs, but also their k distribution quickly stabilizes despite the fact that it is still far from thermal equilibrium. The magnitude of $\langle E_{\rm kin}\rangle$ at $t > 1$ ns was found to decrease nearly linearly with $\delta E_{\rm LP}$.

To study the formation dynamics of spatial coherence in a photoexcited polariton system, we measured the time dependences of the first-order correlation function $g^{(1)}(\mathbf{r}_1, \mathbf{r}_2, t_1 = t_2 = t)$ of polariton emission using time-resolved measurements of the interference of light emitted from different points on the sample. The coherence length L_c was determined from the condition that $g^{(1)} = 1/e$ at the point $\Delta|\mathbf{r}| = L_c$. The increase in $g^{(1)}$ in the decaying LP fluid is connected with decrease in $\langle E_{\rm kin}\rangle$ due to increase in the de Broglie wavelength of polaritons, $\langle\lambda_B\rangle$, and with the suppression of the amplitude and phase fluctuations due to interparticle interaction. To separate the contributions of these effects, the measured dependences of $g^{(1)}(\Delta|\mathbf{r}|, t)$ were compared with the dependences $g^{(1)\star}(\Delta|\mathbf{r}|, t)$, calculated for an incoherent Bose gas with a measured distribution of LPs in momentum space at the corresponding t.

It has been established that in LP fluids with $E_{\rm int} \lesssim 0.05\delta E_{\rm LP}$ the increase in $g^{(1)}$ after the end of the exciting pulse occurs mainly due to the increase in $\langle\lambda_B\rangle$ due to the narrowing of LP distribution in k space. The influence of LP-LP interaction on the formation of long-range spatial coherence in the LP fluid excited in the MC region with $\delta E_{\rm LP} = 0.15$ meV becomes significant at $n_{\rm LP}(t = 0) \approx 7 \times 10^{10}$ cm^{-2}, when $E_{\rm int}$ is about $0.2\delta E_{\rm LP}$. The coherence length in this fluid increases due to partial suppression of amplitude and phase fluctuations at $t = 160$ ps from 3.6 to 5.3 μm, and $g^{(1)}$ at 18.5 μm increases from 0.01 to 0.08.

Simulation of the dynamics of resonantly excited incoherent LPs was carried out with the one-dimensional Schrödinger equation with a random potential. All the main qualitative features of the experimentally studied polariton dynamics were found to be well reproduced within this simplified approximation in comparison with the two-dimensional picture in the experiment. We want to stress that the obtained values for disorder in the effective polariton potential landscape should be considered as qualitative estimations only.

II. EXPERIMENTAL DETAILS

The structure in question was a 2λ-GaAs/AlAs MC grown by molecular beam epitaxy on a GaAs substrate with [100] orientation. The MC contained four sets of three $In_{0.05}Ga_{0.95}As$ quantum wells 10 nm thick separated by 10-nm-thick GaAs barriers. The upper (lower) Bragg mirror consisted of 25 (29) pairs of AlAs and GaAs, which ensured a high quality factor of the MC. The Rabi splitting $R = 7.5$ meV [53–55].

The resonant excitation of the LP fluid was carried out by a mode-locked Ti-sapphire laser generating periodic (80-MHz) pulses with duration 1.5 ps. To break the coherence of the laser beam, we used a 15-m multimode fiber with a core diameter of 400 μm twisted into ten figure-8 loops. The 1.5-ps laser pulses were focused on its input. The 10-ps light pulses coming from the fiber contained a large number of waveguide modes emerging at different angles to form a moiré pattern. To average the moiré pattern in the spatial and angular distributions of the radiation intensity, we used waveguide vibration at a frequency of 50 Hz, which led to a random change in the outgoing waveguide modes during recording of the spectra. The laser pulses were focused along the normal to the MC (z axis) into a 100-μm spot with a near top-hat intensity profile on a sample placed in an optical cryostat in superfluid He at $T = 2$ K. The coherence length of the laser in the excited spot also measured by the interference technique described in [45] did not exceed 2.0 μm.

The resonant excitation of polaritons was carried out at energy $\hbar\omega_p = 1454.1$ meV $= E_{\rm LP}(k = 0) + 0.2$ meV, i.e., approximately 4 meV lower than exciton energy E_X, which made it possible to completely avoid excitation of the exciton reservoir. To excite LPs in a wide range of wave vectors, we used light beams converging in a wide range of angles $2|\mathbf{\Theta}| < 22^\circ$. Light pulses with a large aperture and spectral width generated nonequilibrium polariton fluids with $2|\mathbf{k}| \lesssim 2.5$ μm^{-1}. The LP emission was registered from the central region of an excited spot of 30×30 μm^2. Since the LP emission was

located in the transparency region of the GaAs substrate, it was recorded from the back side of the sample, which made it possible to avoid the contribution from the scattered excitation pulse. The time-resolved emission spectra were measured with a streak camera at time intervals of 450 and 1600 ps with a time resolution of 6 and 21 ps, respectively. They were recorded with an angular resolution of 0.5°, providing a resolution in the k space of $\approx 0.07\ \mu\text{m}^{-1}$.

To measure the dynamics of the spatial coherence of the photoexcited LP fluid, we performed a time-resolved double-slit Young experiment [53]. The central part of the excited spot was imaged at factor 30 magnification on a light-absorbing plate with two pinholes. The interference pattern of the LP radiation coming from the sample sections separated by two pinholes was formed on the slit of a streak camera and recorded with a time resolution of 6 ps. The spatial coherence function $g^{(1)}(x_1, x_2)$ was extracted as the visibility of the interference pattern $g^{(1)}(x_1, x_2) = (I_{\max} - I_{\min})/(I_{\max} + I_{\min})$ where $I_{\max}$ and $I_{\min}$ are minimal and maximal intensities within one period of interference pattern, averaged over all the observed periods.

III. DYNAMICS OF k DISTRIBUTION OF LOW POLARITONS IN AN EXCITED SPOT

Spatial width and In content fluctuations in quantum wells inevitably lead to corresponding fluctuations in the LP resonance energy. Due to the variability of the disorder potential along the sample, the LP emission intensity $I_{\text{LP}}(\mathbf{r})$ in the sample and its angular distribution of $I_{\text{LP}}(\Theta)$ changed as the exciting pulse beam moved along the sample. The amplitude of spatial fluctuations in $I_{\text{LP}}(\mathbf{r})$ in the sample under study, recorded with a spatial resolution of 1.5 μm, reached 50–90%. However, in the sample there were several areas up to 200 μm in size, in which spatial intensity fluctuations did not exceed 15–20% [53].

Figure 1 illustrates a typical time evolution of the spatial and angular distribution of LP emission from the areas with fluctuations within 20%. They were recorded from the central regions of 30×3 and $30 \times 30\ \mu\text{m}^{-2}$, respectively, of a spot with a diameter of 100 μm excited resonantly by incoherent 10-ps pulses converging in a wide range of angles $2|\mathbf{\Theta}| < 15°$ at $\hbar\omega_p = E_{\text{LP}}(k = 0) + 0.2$ meV. Figure 1(a) demonstrates that the spatial fluctuations of the emission intensity of LPs ($t = 10$ ps) generated in this region and, hence, LP densities do not exceed 20%. With increasing delay time relatively small variations in $I_{\text{LP}}(x)$ are observed, which indicates an absence of deep potential traps for LPs in the selected region, hereinafter referred to as region A.

The temporal evolutions of distribution $I_{\text{LP}}(k_x)$ at two pump densities $W_p = 6$ and 0.6 nJ/pulse recorded from the narrow strip in the reciprocal space $|k_y| < 0.1\ \mu\text{m}^{-1}$ are shown in Fig. 1(b). The excited LP densities n_{LP} are equal to $(7 \pm 1) \times 10^{10}$ and $(7 \pm 1) \times 10^{9}\ \text{cm}^{-2}$ at $W_p = 6$ and 0.6 nJ/pulse, respectively. They were determined from the measured powers of integral LP emission $W_{\text{LP}} = 140$ and 14 μW, respectively, as $n_{\text{LP}} = W_{\text{LP}}/E_{\text{LP}} S f_p$, where S is the area of the excited spot and $f_p = 80$ MHz is the pulse repetition frequency. These LP densities are three to four

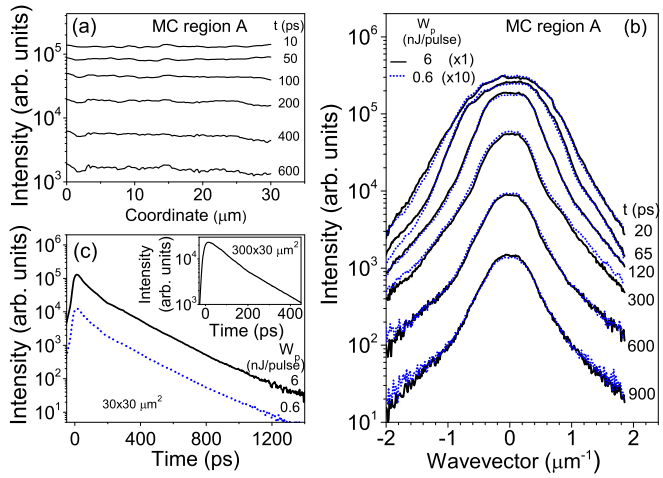

FIG. 1. Time evolution of the spatial (a) and angular (b) distributions of LP emission from the central 30×3 and $30 \times 30\ \mu\text{m}^{-2}$ regions, respectively, of the photoexcited spot with a diameter of 100 μm measured in MC region A. The time dependences of the LP emission intensity from a range of $30 \times 30\ \mu\text{m}^{-2}$ and from a widened range $300 \times 30\ \mu\text{m}^{-2}$ at $W_p = 6$ nJ/pulse are shown in (c) and in the inset in (c), respectively.

orders of magnitude higher than the threshold one for the LP condensation in the excited $L = 100 \times 100\ \mu\text{m}^2$ spot at 2 K, $n_{\text{LP,thr}} = 10^7\ \text{cm}^{-2}$.

Figure 1(b) shows that the normalized temporal evolutions of $I_{\text{LP}}(k_x)$ at $W_p = 6$ and 0.6 nJ/pulse nearly coincide, despite the tenfold difference in the excited n_{LP} values. The full width of $I_{\text{LP}}(k_x)$ at half maximum in the excited LP fluid is $\Delta k_x(t = 10\ \text{ps}) = 1.5 \pm 0.1\ \mu\text{m}^{-1}$. It decreases rapidly in the first 100 ps, which indicates rapid cooling of the nonequilibrium LP fluid in the excited spot. The average kinetic energy of the excited LPs, $\langle E_{\text{kin}} \rangle$, determined from the dependence $I_{\text{LP}}(k_x)$ at $t < 10$ ps using the dispersion law $E_{\text{LP}}(k) = [E_X + E_C(k)]/2 - \sqrt{\{[E_X - E_C(k)]^2 + R^2\}}/2$ is equal to 0.4 ± 0.02 meV. It decreases to 0.33 ± 0.02 meV within the first 100 ps. At $t > 100$ ps, the narrowing of $I_{\text{LP}}(k_x)$ and, consequently, the decrease in $\langle E_{\text{kin}} \rangle$ slow down significantly: during the next 100 ps the decrease in $\langle E_{\text{kin}} \rangle$ is about 0.03 meV, and then during 1 ns $\langle E_{\text{kin}} \rangle$ lies within 0.28 ± 0.03 meV. Note that this $\langle E_{\text{kin}} \rangle$ is 1.7 times greater than $\langle E_{\text{kin}} \rangle$ even in Boltzmann gas with $T_{\text{LP}} = 2$ K.

The rapid cooling of the LP fluid in the excited 100-μm spot immediately after the end of the pump pulse is due to the runaway of the high-energy LPs outside: in the absence of scattering the velocities of LPs $v_{\text{LP}}(k \gtrsim 0.6\ \mu\text{m}^{-1}) = \hbar k/m_{\text{LP}} > 1$ μm/ps. The runaway of the high energy LPs explains also the highly nonexponential decay of $I_{\text{LP}}(t)$ from the excited spot. It is seen in Fig. 1(c) that the decay time of I_{LP} at $t < 50$ ps is less than 90 ps, and only at $t \gtrsim 150$ ps the decay of $I_{\text{LP}}(t)$ becomes exponential with $\tau \approx 170$ ps corresponding to the lifetime of the LPs in the MC.

Figure 1(b) shows that the half width of $I_{\text{LP}}(k_x)$ at half maximum $\Delta k_x/2 \approx 0.4\ \mu\text{m}^{-1}$ remains up to 1 ns, although the runaway time of the nonscattering LPs with $k_x \approx 0.4\ \mu\text{m}^{-1}$ beyond the 100-μm spot is less than 150 ps. Therefore, it is natural to assume that the main reason for the sharp slowdown

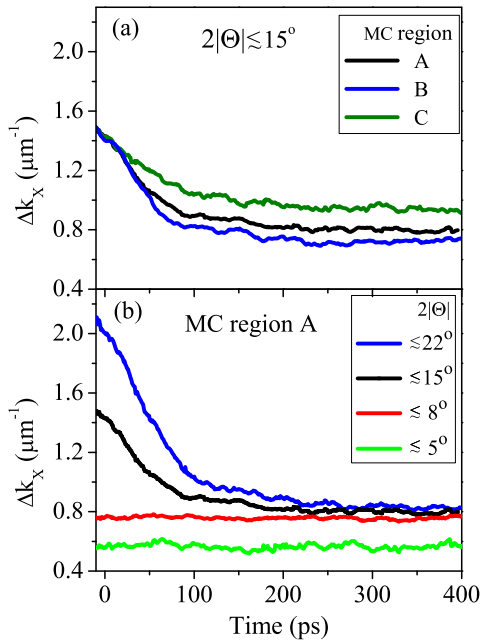

FIG. 2. Experimental dependences of $\Delta k_x(t)$ measured at a fixed aperture of the exciting pulse $2|\mathbf{\Theta}| \lesssim 15^\circ$ ($2|\mathbf{k}| \lesssim 1.8\ \mu\text{m}^{-1}$) from several MC regions (a) and at several $2|\mathbf{\Theta}|$ in the range between 5° and 22° from region *A* (b).

in the narrowing of the k distribution of LPs at $t > 150$ ps is their scattering. The coincidence of the time evolutions of $I_{\text{LP}}(k_x)$ at $W_p = 6$ and 0.6 nJ/pulse indicates that the effect of interparticle scattering of LPs on their dynamics is negligible even at $n_{\text{LP}} = 7 \times 10^{10}\ \text{cm}^{-2}$. This is due to the small magnitude of the LP interaction energy $E_{\text{int}} = \alpha n_{\text{LP}}$ in the investigated MC with 12 quantum wells in the active range. The polariton-polariton interaction constant α is as small as $(4.5 \pm 0.5) \times 10^{-13}\ \text{meV/cm}^2$ because of the distribution of excitons in 12 quantum wells [56]. The magnitudes of E_{int} and $\langle E_{\text{kin}} \rangle$ in the generated fluid at $n_{\text{LP}} = 7 \times 10^{10}\ \text{cm}^{-2}$ are equal to ≈30 and 400 μeV, respectively. With increasing delay time E_{int} in the excited spot decreases about three times during the first 100 ps and then decreases exponentially with $\tau_{\text{LP}} \approx 170$ ps whereas $\langle E_{\text{kin}} \rangle$ decreases in the first 100 ps only by about 30% and then remains nearly constant. As a consequence, the ratio $E_{\text{int}}/\langle E_{\text{kin}} \rangle$ decreases from ≈0.06 at $t = 0$ to less than 0.03 at $t > 100$ ps. Therefore, we assume that the LPs are mainly scattered by the disorder potential caused by random fluctuations in the widths and the In concentration in InGaAs quantum wells.

This conclusion is supported by analysis of the behavior of $\Delta k_x(t)$ in LP fluids generated at fixed angle aperture in MC regions with different spatial fluctuations of $I_{\text{LP}}(\mathbf{r})$ and in one MC region at different angle apertures of the exciting light beam. Figure 2(a) compares the dependences $\Delta k_x(t)$ in the fluid in region *A*, in which spatial fluctuations of the $I_{\text{LP}}(\mathbf{r})$ are within 20%, with $\Delta k_x(t)$ in regions *B* and *C*, in which intensity fluctuations are less than 15% and more than 30%, respectively, in the case of excitation by pulses with the same aperture. It shows that in all the regions the pulses generate fluids with very similar Δk_x whereas the difference in Δk_x established at large t, $\Delta k^\star$, in the small and large disorder regions, reaches nearly 20%.

In contrast, $\Delta k^\star$ in the fluids generated in the same MC region is nearly independent of the pulse aperture until $\Delta k_x(t = 0) > \Delta k^\star$. Figure 2(b) shows that $\Delta k^\star$ decreases less than 4% when $\Delta k_x(t = 0)$ changes three times, from 0.78 to $2.2\ \mu\text{m}^{-1}$. At small pulse apertures when $\Delta k_x(t = 0) < \Delta k^\star \approx 0.8\ \mu\text{m}^{-1}$, the magnitude of $\Delta k_x(t)$ remains nearly constant, which indicates that the mean free path of LPs with $k < \Delta k^\star/2 = 0.4\ \mu\text{m}^{-1}$ ($E_{\text{kin}} \approx 0.1$ meV) is of the order of the excited size $D = 100$ μm. This conclusion agrees well with the small difference in the decay times of I_{LP} in the excited spot at $t \approx 100$ ps and large delay times, $\tau_{\text{LP}} \approx 150$ and 170 ps, respectively.

IV. MOMENTUM SCATTERING TIME OF LOW POLARITONS

More information on momentum scattering time of LPs, τ_k, can be obtained from comparison of the temporal evolution of $I_{\text{LP}}(k_x)$ measured under pumping in a full light cone $2|\mathbf{\Theta}| \leqslant 22^\circ$ ($2|\mathbf{k}| < 2.5\ \mu\text{m}^{-1}$) and in half cones $\Theta_x < 0$ and >0 (sections with $k_x > 0$ and <0, respectively). Figure 3 shows the corresponding dependencies $I_{\text{LP}}(k_x)$ measured for several delay times at $\hbar\omega_p = E_{\text{LP}}(k = 0) + 0.2$ meV in MC region *C*. It is seen that the fraction of LP radiation in the unexcited region k_x monotonically increases with t: it is 1.5 orders of magnitude smaller than in the excited region at $t = 10$ ps and exceeding it slightly at $t > 100$ ps. The scattering of LPs into the unexcited k_x region leads to a faster decrease of their density in the excited k_x region; the sum of $I_{\text{LP}}(k_x)$ measured under pumping at $k_x >$ and <0, as expected, coincides with $I_{\text{LP}}(k_x)$ under pumping by pulses with a full angle cone.

In order to estimate the values of $\tau_k(k)$ from the experimental dependences $I_{\text{LP}}(k_x, t)$ measured under excitation of LPs in a half light cone, we considered that elastic scattering of LPs on the disorder potential occurs without changing $|k|$. As a consequence, the ratio $\rho_k(k, t) = [I_{\text{LP}}(k, t) - I_{\text{LP}}(-k, t)]/[I_{\text{LP}}(k, t) + I_{\text{LP}}(-k, t)]$ in one-dimensional homogeneous LP fluids decreases exponentially with decay time $\tau_k/2$:

$$\rho_k(k, t) = \rho_k(k, t = 0)\exp[-2t/\tau_k(k)]. \tag{1}$$

The dependences $I_{\text{LP}}(k_x, t)$ are measured in a quasi-2D fluid in a very narrow range of $|k_y| < 0.1\ \mu\text{m}^{-1}$. The angular distribution of elastically scattered LPs is random. Formula (1) in this case satisfactorily describes $\rho_k(k_x, t)$ for $k_x \gg |k_y| = 0.1\ \mu\text{m}^{-1}$. Another limitation is related to the finite size $D = 100$ μm of the excited LP fluid as formula (1) is valid only in the limited range of k and t satisfying the condition $v_{\text{LP}}t = \hbar k t/m_{\text{LP}} \lesssim D/2$, i.e., at $t \lesssim 25$ and 50 ps for LPs with $k_x = 0.8$ and $0.4\ \mu\text{m}^{-1}$, respectively.

Figure 4 shows the ratios $\rho_k(k_x, t)$ at $t < 50$ ps extracted from the dependences $I_{\text{LP}}(k_x, t)$ recorded under pumping by light with $k_x > 0$ for MC regions *A* and *C*. It is seen that the dependences $\rho_k(t)$ are well described by formula (1) only in the range of small t, less than ≈30 and 42 ps for LPs with $|k_x| = 0.8$ and $0.4\ \mu\text{m}^{-1}$, respectively. The sharp decrease in ρ_k at longer times is caused by the depletion of the influx into the investigated central 30-μm region of LPs with $k_x > 0$

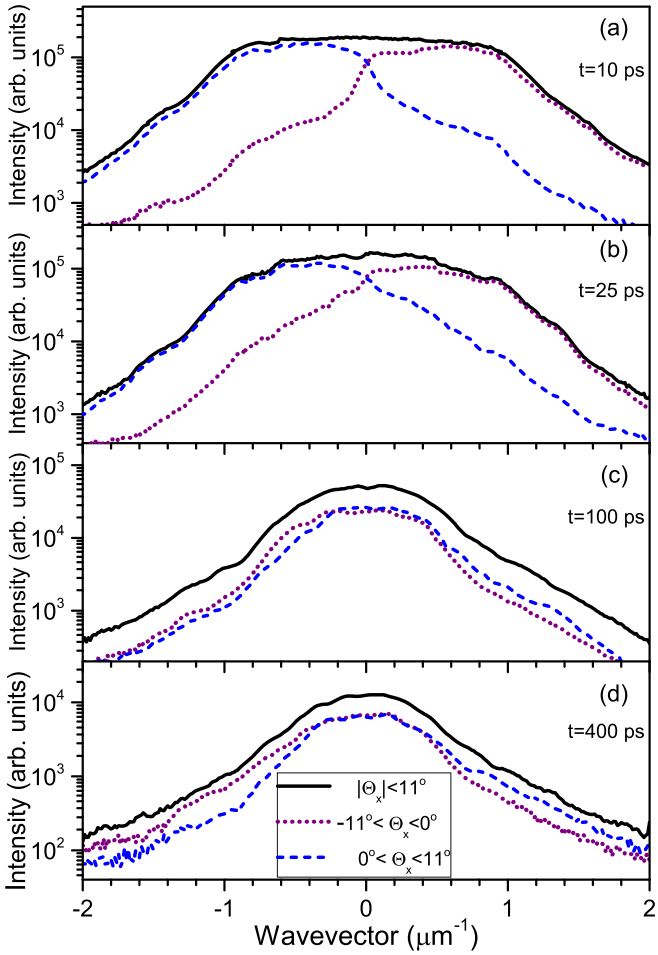

FIG. 3. Time evolution of the angular distribution of LP emission from the central region of 30×30 μm^{-2} of a photoexcited 100-μm spot measured in region C under pumping in a full angle cone $2|\mathbf{\Theta}| \leqslant 22^\circ$ ($2|\mathbf{k}| < 2.5$ μm^{-1}) (black solid line) and in half cones $\Theta_x < 0$ (dotted line) and >0 (dashed line) (sections with $k_x > 0$ and <0, respectively).

excited to the left on it. The extracted values of τ_k in region A are equal to 98 ± 7 and 128 ± 7 ps at $|k_x| = 0.4$ and 0.8 μm^{-1}, respectively. These τ_k values correspond to mean free pass $l_{\rm LP}(k) = v_{\rm LP}\tau_k(k) \approx 65$ and 175 μm, respectively. In region C with a greater disorder they are by about 10% smaller. Such values of $l_{\rm LP}$ explain both the observed quasistabilization of the LP distribution in the k space and evolution of $I_{\rm LP}(t)$ to a monoexponential dependence with $\tau \approx \tau_{\rm LP} = 170$ ps after $\Delta k_x/2$ decreases to $\approx$0.5 μm^{-1}.

V. ESTIMATION OF DISORDER POTENTIAL

The disorder potential $\delta E_{\rm LP}$ in the MC regions is estimated from comparison of measured temporal evolution of $I_{\rm LP}(k)$ with dependences calculated using the linear one-dimensional Schrödinger equation with a random potential. We model the polariton potential landscape by a random function $U(x_i)$ defined on the mesh with step 0.5 μm and characterized by dispersion $\delta E_{\rm LP} = \langle (U - \langle U \rangle)^2 \rangle^{1/2}$. The example of random potential is shown in Fig. 5. The interparticle interaction is neglected as no marked dependence of the LP dynamics on

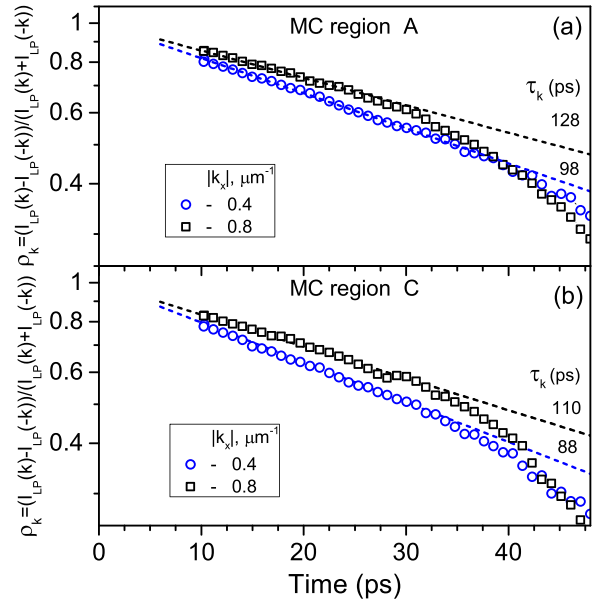

FIG. 4. Experimental ratios $\rho_k(k_x, t)$ at $t < 50$ ps extracted from the dependences $I_{\rm LP}(k_x, t)$ for MC regions A and C (a and b, respectively) recorded under pumping by light with $k_x > 0$. The dashed lines show extrapolation of the dependences with formula (1).

the excitation density was observed at LP densities up to 7×10^{10} cm^{-2}. The initial LP distributions in the real and reciprocal spaces corresponding to those in the experiment are formed under the action of the broadband in the frequency and wave vector excitation pulse in the 100-μm spot. The spectrally limited Gaussian random spectrum corresponds to the spatiotemporal correlation of 1.5 μm and 1.5 ps. The pulse aperture and LP lifetime $\tau_{\rm LP} = 170$ ps are taken from the experiment. The dynamics of the LP fluid is calculated for a large number of random realizations of the exciting pulse with subsequent averaging of the intensity characteristics.

Comparison of $I_{\rm LP}(k_x)$ measured in MC region A (solid lines) with the calculated ones (dotted lines) for several delay

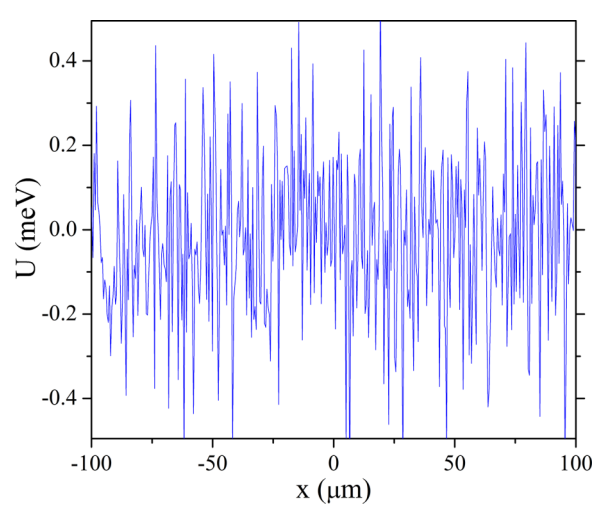

FIG. 5. Example of random potential with $\delta E_{\rm LP} = 0.2$ meV and $\langle U \rangle = 0$ used in the calculations.

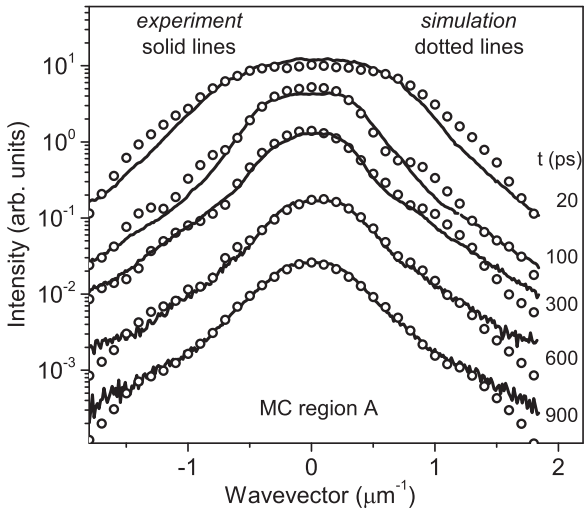

FIG. 6. Comparison of $I_{LP}(k_x)$ measured in MC region A (solid lines) with calculated ones (dotted lines) for several delay times with $\delta E_{LP} = 0.2$ meV.

times with a single adjustable parameter, δE_{LP}, is presented in Fig. 6. The calculated dependences reproduce well both the fast narrowing of $I(k_x)$ in the first 100 ps and the quasistabilization of the k distribution of LPs at large delay times. A noticeable difference is observed only in the range $|k| > 1.4\ \mu m^{-1}$ at large $t \gtrsim 600$ ps where the calculations predict a much faster decrease in $I(k_x)$ with increasing k_x.

To find the reason for this difference we compared the modeled and measured quasistabilized distributions of $I_{LP}(k_x)$ at $t = 0.9$ ns for MC regions with different disorder potentials. The calculated dependences $I_{LP}(k_x)$ are shown in Fig. 7 by dotted lines along with those measured in three MC regions (solid lines). Figure 7 shows that the experimental dependences $I_{LP}(k_x)$ in MC region C with potential disorder close to the average one in the MC are well described in a wide range of $|k_x|$ up to $1.6\ \mu m^{-1}$ at $\delta E_{LP} = 0.32$ meV whereas the deviation of the experimental dependence $I_{LP}(k_x)$ from the calculated one in MC region B with smallest disorder $\delta E_{LP} = 0.15$ meV begins already at $|k| \approx 1\ \mu m^{-1}$. Note also the small difference in the fraction of LPs with $k > 1.4\ \mu m^{-1}$ in the MC regions with high and low disorder in measured $I_{LP}(k_x)$. These facts indicate that the deviation of the measured dependences from the calculated ones can be well explained by the nonhomogeneity of the potential disorder in the MC. Indeed, the lateral size of the investigated 100-μm regions with small disorder is much smaller than the mean free pass of LPs with $k > 1\ \mu m^{-1}$. As a result, the dynamics of LPs with large k in MC regions A and B is determined mainly by their scattering outside the excited spot with greater disorder.

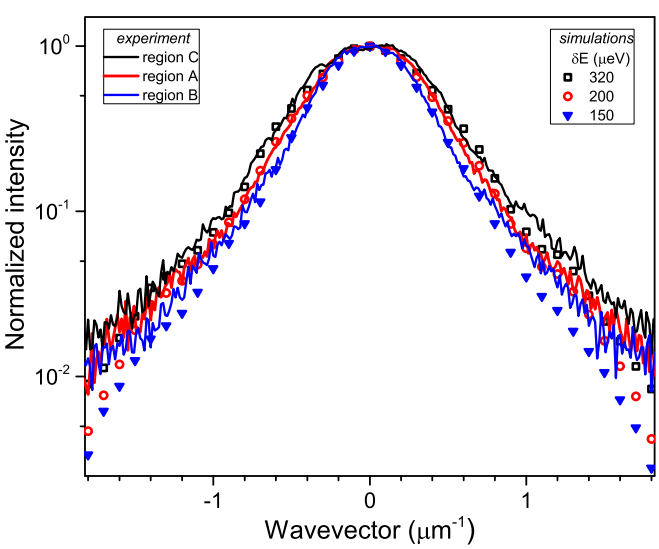

FIG. 7. Comparison of measured quasistabilized dependences $I_{LP}(k_x)$ (solid lines) at $t = 0.9$ ns with calculated ones (dotted lines) in three MC regions with different disorder potentials.

Thus, despite the obvious simplified one-dimensional approximation in the calculations compared with the two-dimensional picture in the experiment, the calculated dependences $I_{LP}(k_x, t)$ reproduce all the main features of the measured polariton dynamics such as the fast narrowing of the k distribution of the photoexcited LPs after the end of the excitation pulse, the well-pronounced slowdown of this process at $t \gtrsim 100$ ps, and the very slow variation ("quasistabilization") of $n_{LP}(k)$ at delay times $t \gtrsim 200$ ps.

VI. COHERENCE EXPANSION IN THE DENSE NONCOHERENT LP FLUID

The formation of a condensate state in a free LP system still remains one of the open questions. The incoherent LP fluid photoexcited in our experiment has a density of $n_{LP} \approx 7 \times 10^{10}\ cm^{-2}$, which exceeds the LP condensation threshold at 2 K by more than three orders of magnitude and is very far from thermal equilibrium. The particle condensation in a nonequilibrium gas is determined by three processes with different time scales [57,58]. The first is gas cooling, leading to an increase in the fraction of particles in the so-called coherent region where the kinetic energy of a particle is of the order of its interaction energy with other particles. The second is the smoothing of the density fluctuations, leading to the formation of quasicondensate. Finally, the third is the smoothing of the phase fluctuations, meaning the onset of a "true condensate." The quasicondensate amplitude fluctuations are suppressed during the time $\tau_s \sim \hbar/E_{int}$.

Figure 8 shows that $n_{LP}(E_{kin})$ in the generated fluid decreases nearly exponentially over a wide range of $E_{kin} < 1.2$ meV without any noticeable peak near the band bottom characteristic of the condensed phase, despite the fact that this density exceeds the critical density for Bose-Einstein condensation by more than three orders of magnitude. The dependence of the ratio $n_{LP}(E_{kin})/n_{LP}(E_{kin} = 0)$ is close to the Boltzmann one with an effective temperature of 4.4 K, which proves that the generated LP fluid, despite the presence of a significant fraction of polaritons near the LP band bottom, does not contain a noticeable condensate fraction at $k = 0$. At the same time, it should be noted that, owing to the very high density of LPs, E_{int} is much greater than in a thermal Boltzmann gas. In particular, $E_{int} \approx 30$ μeV for $n_{LP} = 7 \times 10^{10}\ cm^{-2}$ and the percentage of particles with $E_{kin} < 30$ μeV is about 7%.

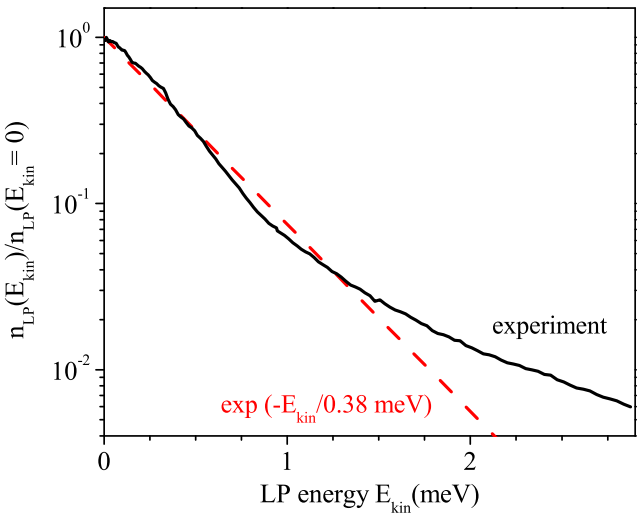

FIG. 8. Energy distribution of LPs in the LP fluid generated at $W_p = 6$ nJ/pulse.

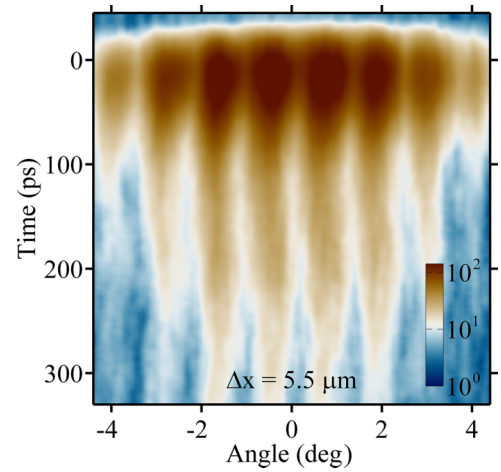

FIG. 9. Time dependence of the interferogram of the LP emission measured in the time-resolved double-slit Young experiment in region B at $\Delta x = 5.5$ μm and $W_p = 6$ nJ/pulse.

The cooling of the excited LP fluid is determined by the LP relaxation into the low-energy region due to the processes of scattering and/or escape of high-energy LPs outward. As was established in Sec. III, the cooling rates of the LP fluids with $n_{\rm LP}(t=0) = 7\times10^{10}$ cm^{-2} and 7×10^{9} cm^{-2} at 2 K are the same. The predominant cooling mechanism is the runaway of the high-energy LPs beyond the excited spot. The cooling rate slows down as t increases. After the fluid expands at $t \approx 100$ ps up to the size of the order of the mean free path of LPs, the decrease in $\langle E_{\rm kin}\rangle$ over the next 300 ps does not exceed 12%.

We have studied the time dependences of the first-order spatial coherence function $g^{(1)}(\Delta x, t)$ by measuring the interference of light emitted from different points of the sample. We have found that the interference patterns of the LP emission measured from two spots with a diameter of 1.5 μm separated by $\Delta x \leqslant 18.5$ μm in the regions with different potential disorder show the greatest visibility of interference fringes in region B with the smallest disorder.

Figure 9 shows a streak camera image of the temporal behavior of the interference pattern of the LP emission in region B from two points separated by $\Delta x = 5.5$ μm at $W_p =$ 6 nJ/pulse. The horizontal axis corresponds to the angle of emission passing through the pinholes, relative to the sample normal. It can be seen that the visibility of the interference fringes in the double-slit experiment is very small during the excitation pulse ($t \lesssim 10$ ps),then increases monotonically at $t \lesssim 160$ ps, which indicates a gradual increase in the spatial coherence of the LP fluid, and afterwards changes very slowly. Supplemental Material [53] contains sets of dependences of the emission intensity at several $t \leqslant 270$ ps in the central strip of the interference pattern along the x axis, normalized to the total intensity from two pinholes ($I_1^{\rm PH} + I_2^{\rm PH}$), for three distances between their centers $\Delta x = 5.5$, 8.5, and 15.5 μm.

The first-order spatial correlation functions $g^{(1)}(\Delta x)$ in the exciting pulse and in the LP fluid with $n_{\rm LP}(t=0) = 7\times 10^{10}$ cm^{-2} at different delay times over the range $t \leqslant 270$ ps, determined from the measured interferogram, are presented in Fig. 10, along with the functions $g^{(1)\star}(\Delta x)$ calculated for a classical incoherent gas with $n_{\rm LP}(k)$ that is equal to one measured at the corresponding delay times. $g^{(1)\star}(\Delta x)$ are calculated from the measured dependences $n_{\rm LP}(k)$ [29] as

$$g^{(1)\star}(\mathbf{r}) = \sum_{\mathbf{k}} n_{\rm LP}(\mathbf{k})\exp(i\mathbf{kr}) \Big/ \sum_{\mathbf{k}} n_{\rm LP}(\mathbf{k}). \qquad (2)$$

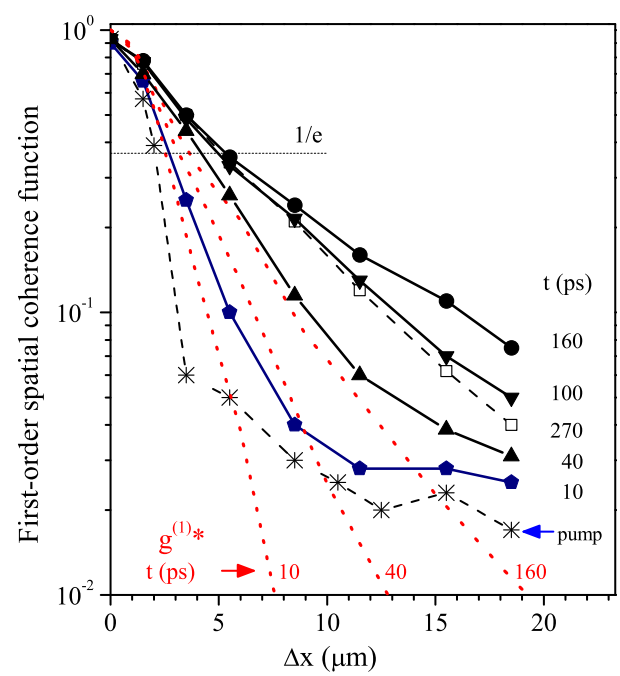

FIG. 10. Comparison of experimental dependences $g^{(1)}(\Delta x)$ in the LP fluid generated in region B by pulses with $W_p = 6$ nJ/pulse at several $t \leqslant 270$ ps (lines with symbols) with dependences $g^{(1)\star}(\Delta x)$ calculated for a classical noninteracting gas with measured dependences $n_{\rm LP}(k_x)$ (red dashed lines). The dashed line with crosses represents the measured dependence $g^{(1)}_{\rm pump}(\Delta x)$ in the excited laser spot.

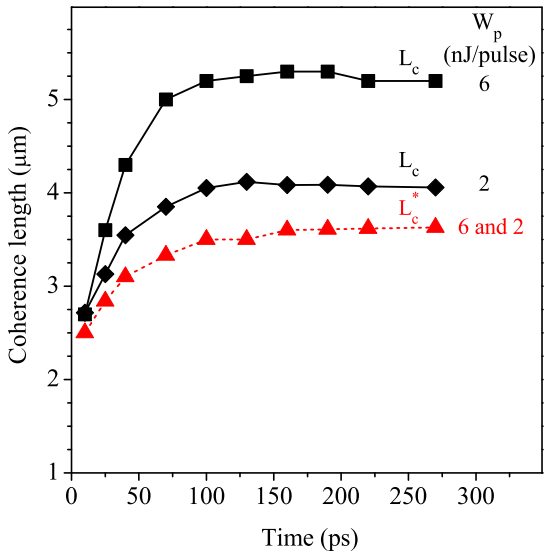

FIG. 11. Time dependencies of L_c determined from $g^{(1)}$ and L_c^* determined from $g^{(1)\star}$ at $W_p = 6$ and 2 nJ/pulse.

In a homogeneous system of LPs with isotropic k distribution,

$$g^{(1)\star}(x) = \int_{1/L}^{\infty} n_{\mathrm{LP}}(k) J_0(kx) k dk \Big/ \int_{1/L}^{\infty} n_{\mathrm{LP}}(k) k dk \qquad (3)$$

where J_0 is the zeroth-order Bessel function and L is the lateral size.

The correlation function $g^{(1)}_{\mathrm{pump}}(\Delta x)$ in Fig. 10 shows that the coherence length in the pump laser beam after passing through a long 8-shaped waveguide decreases to 2.0 ± 0.2 μm. However, $g^{(1)}_{\mathrm{pump}}$ does not tend to zero for large Δx. It remains close to 0.02 over a wide range up to 19 μm, indicating that the pulse retains a small, about 2%, coherent component.

Figure 10 shows that the experimental dependence $g^{(1)}$ at $t = 10$ ps and the dependence $g^{(1)\star}$ calculated for an incoherent gas using Eq. (3) and $n_{\mathrm{LP}}(k_x)$ for $t = 10$ ps are very close to each other at $\Delta x < 3$ μm. Time dependences of L_c determined from $g^{(1)}$ and L_c^* determined from $g^{(1)\star}$ at $W_p = 6$ and 2 nJ/pulse are shown in Fig. 11. It is seen that L_c and L_c^* at $t = 10$ ps are equal to 2.7 ± 0.2 and 2.5 ± 0.2 μm, respectively. These values slightly exceed $L_c = 2.0$ μm in the exciting pulse, which is apparently caused by a decrease in the efficiency of the LP excitation at large k due to an increase in the exciton component. The noticeable discrepancy between $g^{(1)}$ and $g^{(1)\star}$ at large Δx is due to the presence of a small coherent fraction inherited from the exciting beam. Indeed, the dependence $g^{(1)}(\Delta x)$ after subtracting the 2.8% contribution of the coherent fraction coincides with $g^{(1)*}(\Delta x)$.

We emphasize that the coherence fraction in the LP fluid, inherited from the exciting pulse, is not a condensate at the LP band bottom: it, as in the exciting light beam, includes all k states, and not just states from the coherent region with $E_{\mathrm{kin}} < E_{\mathrm{int}}$. As already discussed above, $n_{\mathrm{LP}}(E_{\mathrm{kin}})$ at $t = 10$ ps decreases nearly exponentially without any noticeable peak near the band bottom, which would be characteristic of the condensate at $k \approx 0$. Note also that this conclusion is confirmed by our measurements of $g^{(1)}$ in the fluids resonantly excited above $E_{\mathrm{LP}}(k = 0)$ in the range of wave vectors $0.3 < |k| < 2$ μm^{-1} ($E_{\mathrm{kin}} > 70$ μeV $\approx 2E_{\mathrm{int}}$), which showed that the percentage of the coherent fraction in this fluid also remains close to 2.5%. Thus, the fluid under study is very close to the classical highly nonequilibrium incoherent gas with a small (7%) fraction of polaritons in the coherent region.

The dependencies of coherence lengths $L_c(t)$ and $L_c^\star(t)$, determined, respectively, from measured $g^{(1)}(\Delta x, t)$ and calculated $g^{(1)\star}$ at $W_p = 6$ and 2 nJ/pulse are shown in Fig. 11. $L_c^\star(t)$ at these W_p coincide due to the equivalence, within the measurement error, of the measured $n_{\mathrm{LP}}(k, t)$. At the same time, Fig. 11 shows that (i) the measured L_c grow at small t noticeably faster than $L_c^\star$ and (ii) L_c at $W_p = 6$ nJ/pulse is markedly greater than at 2 nJ/pulse. The faster growth of L_c can naturally be explained by the effect of smoothing fluctuations in the fluid density owing to the LP-LP interaction. That means that the influence of the LP-LP interaction in the presence of the disorder manifests itself in the formation of spatial coherence of LPs at markedly smaller LP densities than in their redistribution in the reciprocal space.

The maximum values of L_c at $W_p = 2$ and 6 nJ/ps are achieved at $t \approx 100$ and 160 ps, respectively. They exceed the $L_c^\star$ calculated for an incoherent gas at the corresponding t by 0.6 and 1.7 μm, respectively. For longer delay times L_c decreases slowly and approaches $L_c^\star$. The decrease in L_c during 100 ps is about 3%. The long decoherence time in LP systems is associated with the inefficiency of the acoustic-phonon assisted scattering of photonlike LPs at helium temperatures and has already been discussed in a number of studies [32,46,59–61].

It is of interest to follow the dynamics of the coherence fraction inherited from the exciting pulse in the fluid with $n_{\mathrm{LP}}(t = 0) \approx 7 \times 10^{10}$ cm^{-2}. At $t = 10$ ps this fraction determines a nearly constant $g^{(1)} = 0.028$ in the entire range $11 < \Delta x < 18.5$ μm. If the stimulated scattering in this fraction played a dominant role in the formation of spatial coherence in the fluid, one would expect the same rate of increase in $g^{(1)}$ throughout this region. However, Fig. 10 shows that the rate of its growth with t quickly decreases with increasing Δx. Thus, $g^{(1)}(t = 40$ ps) at $\Delta x = 18.5$ μm increases by 0.005, while at $\Delta x = 11.5$ μm it increases six times more, by 0.03, and a comparison of $g^{(1)}(\Delta x)$ and $g^{(1)\star}(\Delta x)$ shows that only half of this increase may be attributed to the effect of the fluid cooling. Therefore, we can conclude that the presence of a small coherent component inherited from the exciting pulse has virtually no effect on the formation of spatial coherence in the fluid under study.

Finally, we note that the influence of an LP-LP interaction on the formation of long-range spatial coherence in the LP fluid at large Δx can be assessed from a comparison of the measured dependences $g^{(1)}(\Delta x)$ with $g^{(1)\star}(\Delta x)$ calculated for a classical incoherent gas with measured dependences $n_{\mathrm{LP}}(k_x)$. Figure 10 shows that $g^{(1)}(t = 160$ ps) at $\Delta x \geqslant 15.5$ μm is approximately seven times greater than $g^{(1)\star}$. Consequently, the development of long-range coherence in the fluid at these Δx is determined by the LP-LP interaction. The growth rate of $g^{(1)}(\Delta x = 15.5$ μm) does not exceed 1 ns^{-1}, whereas an expected smoothing rate of density and phase fluc-

tuations in a classical Bose gas with a similar $E_{\rm int} \approx 30$ μeV in the absence of disorder is of the order $E_{\rm int}/\hbar \approx 10\ {\rm ns}^{-1}$. An increase in τ_s in LP fluids in the disordered potential is well expected because of a weakening of interaction of particles separated by potential barriers in the random potential.

Thus, the experiment shows that the influence of the LP-LP interaction in the presence of the disorder manifests itself in the formation of the spatial coherence of LPs at markedly smaller LP densities than in their redistribution in reciprocal space. The presented linear theoretical model describes the temporal evolution of the polariton's spectral characteristics in the LP fluids with $E_{\rm int}$ smaller than $0.2\delta E_{\rm LP}$, but the theoretical description of coherence formation is far beyond its capabilities. The presented experimental observations of the disorder-interaction interplay require further theoretical studies.

VII. CONCLUSION

We have studied the time evolution of a nonequilibrium incoherent *really* free LP fluid resonantly excited in a high-Q planar 2λ GaAs/AlAs MC containing 12 InGaAs quantum wells. The fluid was resonantly excited in a 100-μm spot with nearly top-hat intensity profile at 2 K in a wide range of $2|\mathbf{k}| \lesssim 2.5\ \mu{\rm m}^{-1}$ with an average LP kinetic energy $\langle E_{\rm kin}\rangle = 0.4$ meV using incoherent converging picosecond optical pulses. The LP decay time of $\tau_{\rm LP} \approx 170$ ps made it possible to study the LP dynamics during 1.5 ns.

It is found that the k distribution of LPs in the excited spot narrows rapidly after termination of the excitation pulse. This narrowing is caused by the runaway of the high-energy LPs beyond the excited region. It continues until the fluid expands to a size on the order of the LP mean free path, which gradually decreases with increasing potential disorder. Afterwards, the k distribution stabilizes, even though it is still far from thermal equilibrium. Moreover, the time dependence of $n_{\rm LP}(k_x, t)$ is independent of the excitation density up to $n_{LP}(t = 0) \approx 7 \times 10^{10}\ {\rm cm}^{-2}$ and is well described in terms of the linear Schrödinger equations, taking into account only the random disorder potential and finite lifetime. We stress that this $n_{\rm LP}$ exceeds the Bose-Einstein condensation threshold at 2 K by more than three orders of magnitude. The weak influence of the interparticle interaction is explained by the smallness of $E_{\rm int}/\langle E_{\rm kin}\rangle$ in the decaying LP fluid: this ratio in a fluid with $n_{\rm LP} = 7 \times 10^{10}\ {\rm cm}^{-2}$ is equal to approximately 0.06 and gradually decreases with time in the decaying fluid.

Measurements of the time dependences of $g^{(1)}(\Delta x)$ showed that potential disorder in MCs leads to a slowdown in the formation of long-range spatial coherence in a cavity LP fluid compared to that in a classical Bose gas in the absence of the potential disorder, in which the smoothing time of density and phase fluctuations is determined only by $E_{\rm int}$. The dynamics of the distribution of polaritons in k space and the time evolution of $g^{(1)}(\Delta x)$ were independently measured in order to identify the reason for the slowdown in the formation of a polariton condensate. Based on a comparison of the measured dependences $g^{(1)}(\Delta x)$ and the dependences $g^{(1)\star}(\Delta x)$ calculated for a classical incoherent gas with the measured dependences $n_{\rm LP}(k_x)$, we determined the contributions to $g^{(1)}$ due to the cooling of the polariton system (a decrease in $\langle E_{\rm kin}\rangle$) and due to the smoothing of density and phase fluctuations due to interparticle interaction.

As expected, the contribution of interparticle interaction in $g^{(1)}$ is found to be insignificant as long as $E_{\rm int} \ll \delta E_{\rm LP}$, but it becomes pronounced already at $E_{\rm int} \approx 0.2\delta E_{\rm LP}$, when its influence on the k distribution of LPs remains insignificant. In particular, L_c at $t = 160$ ps in a dense fluid with $n_{\rm LP}(t = 0) = 7 \times 10^{10}\ {\rm cm}^{-2}$ in the region with $\delta E_{\rm LP} = 0.15$ meV exceeds $L_c^\star$ calculated for a classical incoherent gas with the same $n_{\rm LP}(k)$ by 1.5 times (5.3 and 3.6 μm, respectively). The presented linear theoretical model well describes the LP dynamics in the k space for $E_{\rm int} \lesssim 0.2\delta E_{\rm LP}$, but the theoretical description of coherence formation in this range goes far beyond its capabilities.

The presented results are important for understanding the formation of long-range coherence both in purely polariton systems in MCs, and in other gases of Bose quasiparticles in low-dimensional structures with potential disorder. They can be useful in the practical use of cavity polaritons in quantum devices, since the potential disorder is always present in semiconductor MCs due to fluctuations in the width of quantum wells in the active region, and disorder parameters can vary significantly in the sample plane. A deep understanding of the influence of disorder on the spectra and dynamics of polaritons is especially necessary in the case of high-Q MCs, when quasilocalized LP levels become spectrally resolved and the inhomogeneously broadened LP level breaks up into a set of narrow sublevels controlled by the local structure of potential disorder. High rates of condensate formation in such systems in the case of excitation below the inflection point can only be achieved when $E_{\rm int}$ is greater than $\delta E_{\rm LP}$.

ACKNOWLEDGMENTS

We are grateful to S. S. Gavrilov, S. G. Tikhodeev, and V. B. Timofeev for fruitful discussions and to P. G. Savvidis for the sample with a high-Q MC. The work was supported by Russian Science Foundation Grant No. 21-12-00368.

[1] J. Kasprzak, M. Richard, S. Kundermann, A. Baas, P. Jeambrun, J. M. J. Keeling, F. M. Marchetti, M. H. Szymanska, R. Andre, J. L. Staehli, V. Savona, P. B. Littlewood, B. Deveaud, and L. S. Dang, Bose-Einstein condensation of exciton polaritons, Nature (London) **443**, 409 (2006).

[2] R. Balili, V. Hartwell, D. Snoke, L. Pfeiffer, and K. West, Bose-Einstein condensation of microcavity polaritons in a trap, Science **316**, 1007 (2007).

[3] Hui Deng Gregor Weihs, C. Santori, J. Bloch, and Y. Yamamoto, Condensation of semiconductor microcavity exciton polaritons, Science **298**, 199 (2002).

[4] H. Deng, G. S. Solomon, R. Hey, K. H. Ploog, and Y. Yamamoto, Spatial coherence of a polariton condensate, Phys. Rev. Lett. **99**, 126403 (2007).

[5] H. Deng, H. Haug, and Y. Yamamoto, Exciton-polariton Bose-Einstein condensation, Rev. Mod. Phys. **82**, 1489 (2010).

[6] S. Christopoulos, G. Baldassarri Höger von Högersthal, A. J. D. Grundy, P. G. Lagoudakis, A. V. Kavokin, J. J. Baumberg, G. Christmann, R. Butte, E. Feltin, J.-F. Carlin, and N. Grandjean, Room-temperature polariton lasing in semiconductor microcavities, Phys. Rev. Lett. **98**, 126405 (2007).

[7] J. Levrat, R. Butte, E. Feltin, J.-F. Carlin, N. Grandjean, D. Solnyshkov, and G. Malpuech, Condensation phase diagram of cavity polaritons in GaN-based microcavities: Experiment and theory, Phys. Rev. B **81**, 125305 (2010).

[8] F. Li, L. Orosz, O. Kamoun, S. Bouchoule, C. Brimont, P. Disseix, T. Guillet, X. Lafosse, M. Leroux, J. Leymarie, M. Mexis, M. Mihailovic, G. Patriarche, F. Reveret, D. Solnyshkov, J. Zuniga-Perez, and G. Malpuech, From Excitonic to photonic polariton condensate in a ZnO-based microcavity, Phys. Rev. Lett. **110**, 196406 (2013).

[9] S. Kena-Cohen and S. R. Forrest, Room-temperature polariton lasing in an organic single-crystal microcavity, Nat. Photonics **4**, 371 (2010).

[10] T. Byrnes, N. Kim, and Y. Yamamoto, Exciton-polariton condensates, Nat. Phys. **10**, 803 (2014).

[11] X. Zhang, Y. Zhang, H. Dong, B. Tang, D. Li, C. Tian, C. Xua, and W. Zhou, Room temperature exciton-polariton condensate in an optically-controlled trap, Nanoscale **11**, 4496 (2019).

[12] R. Su, S. Ghost, J. Wang, S. Liu, C. Diederichs, T. C. H. Liew, and Q. Xiong, Observation of exciton polariton condensation in a perovskite lattice at room temperature, Nat. Phys. **16**, 301 (2020).

[13] M. Dusel, S. Betzold, O. A. Egorov, S. Klembt, J. Ohmer, U. Fisher, S. Höfling, and C. Schneider, Room temperature organic exciton-polariton condensate in a lattice, Nat. Commun. **11**, 2863 (2020).

[14] L. C. Flatten, Z. He, D. M. Coles, A. A. P. Trichet, A. W. Powell, R. A. Taylor, J. H. Warner, and J. M. Smith, Room-temperature exciton-polaritons with two-dimensional WS_2, Sci. Rep. **6**, 33134 (2016).

[15] C. Anton-Solanas, M. Waldherr, M. Klaas, H. Suchomel, T. H. Harder, H. Cai, E. Sedov, S. Klembt, A. V. Kavokin, S. Tongay, K. Watanabe, T. Taniguchi, S. Höfling, and C. Schneider, Bosonic condensation of exciton-polaritons in an atomically thin crystal, Nat. Mater. **20**, 1233 (2021).

[16] M. Wei, W. Verstraelen, K. Orfanakis, A. Ruseckas, T. C. H. Liew, I. D. W. Samuel, G. A. Turnbull, and H. Ohadi, Optically trapped room temperature polariton condensate in an organic semiconductor, Nat. Commun. **13**, 7191 (2022).

[17] A. Kavokin, J. J. Baumberg, G. Malpuech, and F. P. Laussy, *Microcavities* (Oxford University, New York, 2011).

[18] M. Vladimirova, S. Cronenberger, D. Scalbert, K. V. Kavokin, A. Miard, A. Lemaitre, J. Bloch, D. Solnyshkov, G. Malpuech, and A. V. Kavokin, Polariton-polariton interaction constants in microcavities, Phys. Rev. B **82**, 075301 (2010).

[19] N. Takemura, S. Trebaol, M. Wouters, M. T. Portella-Oberli, and B. Deveaud, Heterodyne spectroscopy of polariton spinor interactions, Phys. Rev. B **90**, 195307 (2014).

[20] A. Amo, T. C. H. Liew, C. Adrados, R. Houdre, E. Giacobino, A. V. Kavokin, and A. Bramati, Exciton-polariton spin switches, Nat. Photonics **4**, 361 (2010).

[21] D. Ballarini, M. De Giorgi, E. Cancellieri, R. Houdre, E. Giacobino, R. Cingolani, A. Bramati, G. Gigli, and D. Sanvitto, All-optical polariton transistor, Nat. Commun. **4**, 1778 (2013).

[22] F. Marsault, H. S. Nguyen, D. Tanese, A. Lemaitre, E. Galopin, I. Sagnes, A. Amo, and J. Bloch, Realization of an all optical exciton-polariton router, Appl. Phys. Lett. **107**, 201115 (2015).

[23] L. Pickup, K. Kalinin, A. Askitopoulos, Z. Hatzopoulos, P. G. Savvidis, N. G. Berloff, and P. G. Lagoudakis, Optical bistability under nonresonant excitation in spinor polariton condensates, Phys. Rev. Lett. **120**, 225301 (2018).

[24] A. Kavokin, T. C. H. Liew, C. Schneider, P. G. Lagoudakis, S. Klembt, and S. Höefling, Polariton condensates for classical and quantum computing, Nat. Rev. Phys. **4**, 435 (2022).

[25] G. Nardin, K. G. Lagoudakis, M. Wouters, M. Richard, A. Baas, R. Andre, Le Si Dang, B. Pietka, and B. Deveaud-Pledran, Dynamics of long-range ordering in an exciton-polariton condensate, Phys. Rev. Lett. **103**, 256402 (2009).

[26] H. Ohadi, E. Kammann, T. C. H. Liew, K. G. Lagoudakis, A. V. Kavokin, and P. G. Lagoudakis, Spontaneous symmetry breaking in a polariton and photon laser, Phys. Rev. Lett. **109**, 016404 (2012).

[27] B. Nelsen, G. Liu, M. Steger, D. W. Snoke, R. Balili, K. West, and L. Pfeiffer, Dissipationless flow and sharp threshold of a polariton condensate with long lifetime, Phys. Rev. X **3**, 041015 (2013).

[28] A. V. Larionov, V. D. Kulakovskii, S. Höfling, C. Schneider, L. Worschech, and A. Forchel, Polarized nonequilibrium Bose-Einstein condensates of spinor exciton polaritons in a magnetic field, Phys. Rev. Lett. **105**, 256401 (2010).

[29] V. V. Belykh, N. N. Sibeldin, V. D. Kulakovskii, M. M. Glazov, M. A. Semina, C. Schneider, S. Höfling, M. Kamp, and A. Forchel, Coherence expansion and polariton condensate formation in a semiconductor microcavity, Phys. Rev. Lett. **110**, 137402 (2013).

[30] F. Tassone and Y. Yamamoto, Exciton-exciton scattering dynamics in a semiconductor microcavity and stimulated scattering into polaritons, Phys. Rev. B **59**, 10830 (1999).

[31] G. Malpuech, A. Kavokin, A. Di Carlo, and J. J. Baumberg, Polariton lasing by exciton-electron scattering in semiconductor microcavities, Phys. Rev. B **65**, 153310 (2002).

[32] T. D. Doan, H. T. Cao, D. Thoai, and H. Haug, Condensation kinetics of microcavity polaritons with scattering by phonons and polaritons, Phys. Rev. B **72**, 085301 (2005).

[33] H. Deng, D. Press, S. Götzinger, G. S. Solomon, R. Hey, K. H. Ploog, and Y. Yamamoto, Quantum degenerate exciton-polaritons in thermal equilibrium, Phys. Rev. Lett. **97**, 146402 (2006).

[34] F. Manni, K. G. Lagoudakis, B. Pietka, L. Fontanesi, M. Wouters, V. Savona, R. Andre, and B. Deveaud-Pledran, Polariton condensation in a one-dimensional disordered potential, Phys. Rev. Lett. **106**, 176401 (2011).

[35] A. Trichet, E. Durupt, F. Medard, S. Datta, A. Minguzzi, and M. Richard, Long-range correlations in a 97% excitonic one-dimensional polariton condensate, Phys. Rev. B **88**, 121407(R) (2013).

[36] J. Schmutzler, T. Kazimierczuk, O. Bayraktar, M. Assmann, M. Bayer, S. Brodbeck, M. Kamp, C. Schneider, and S. Höfling, Influence of interactions with noncondensed particles on the coherence of a one-dimensional polariton condensate, Phys. Rev. B **89**, 115119 (2014).

[37] G. Malpuech, D. D. Solnyshkov, H. Ouerdane, M. M. Glazov, and I. Shelykh, Bose glass and superfluid phases of cavity polaritons, Phys. Rev. Lett. **98**, 206402 (2007).

[38] A. Baas, K. G. Lagoudakis, M. Richard, R. Andre, L. S. Dang, and B. Deveaud-Pledran, Synchronized and desynchronized phases of exciton-polariton condensates in the presence of disorder, Phys. Rev. Lett. **100**, 170401 (2008).

[39] L. Fontanesi, M. Wouters, and V. Savona, Superfluid to bose-glass transition in a 1D weakly interacting bose gas, Phys. Rev. Lett. **103**, 030403 (2009).

[40] D. Sanvitto and V. Timofeev, *Exciton Polaritons in Microcavities* (Springer-Verlag, Berlin, 2012).

[41] A. Askitopoulos, H. Ohadi, A. V. Kavokin, Z. Hatzopoulos, P. G. Savvidis, and P. G. Lagoudakis, Polariton condensation in an optically induced two-dimensional potential, Phys. Rev. B **88**, 041308(R) (2013).

[42] Y. Sun, P. Wen, Y. Yoon, G. Liu, M. Steger, L. N. Pfeiffer, K. West, D. W. Snoke, and K. A. Nelson, Bose-Einstein condensation of long-lifetime polaritons in thermal equilibrium, Phys. Rev. Lett. **118**, 016602 (2017).

[43] A. Askitopoulos, T. C. H. Liew, H. Ohadi, Z. Hatzopoulos, P. G. Savvidis, and P. G. Lagoudakis, Robust platform for engineering pure-quantum-state transitions in polariton condensates, Phys. Rev. B **92**, 035305 (2015).

[44] K. Orfanakis, A. F. Tzortzakakis, D. Petrosyan, P. G. Savvidis, and H. Ohadi, Ultralong temporal coherence in optically trapped exciton-polariton condensates, Phys. Rev. B **103**, 235313 (2021).

[45] A. A. Demenev, Ya. V. Grishina, S. I. Novikov, V. D. Kulakovskii, C. Schneider, and S. Höfling, Loss of coherence in cavity-polariton condensates: Effect of disorder versus exciton reservoir, Phys. Rev. B **94**, 195302 (2016).

[46] A. A. Demenev, Ya. V. Grishina, A. V. Larionov, N. A. Gippius, C. Schneider, S. Höfling, and V. D. Kulakovskii, Polarization instability and the nonlinear internal Josephson effect in cavity polariton condensates generated in an excited state in gaas microcavities of lowered symmetry, Phys. Rev. B **96**, 155308 (2017).

[47] O. Penrose and L. Onsager, Bose-Einstein condensation and liquid helium, Phys. Rev. **104**, 576 (1956).

[48] Roy J. Glauber, Coherent and incoherent states of the radiation field, Phys. Rev. **131**, 2766 (1963).

[49] E. Wertz, L. Ferrier, D. D. Solnyshkov, R. Johne, D. Sanvitto, A. Lemaitre, I. Sagnes, R. Grousson, A. V. Kavokin, P. Senellart, G. Malpuech, and J. Bloch, Spontaneous formation and optical manipulation of extended polariton condensates, Nat. Phys. **6**, 860 (2010).

[50] M. Wouters, Energy relaxation in the mean-field description of polariton condensates, New J. Phys. **14**, 075020 (2012).

[51] M. Pieczarka, M. Boozarjmehr, E. Estrecho, Y. Yoon, M. Steger, K. West, L. N. Pfeiffer, K. A. Nelson, D. W. Snoke, A. G. Truscott, and E. A. Ostrovskaya, Effect of optically induced potential on the energy of trapped exciton polaritons below the condensation threshold, Phys. Rev. B **100**, 085301 (2019).

[52] M. Pieczarka, O. Bleu, E. Estrecho, M. Wurdack, M. Steger, D. W. Snoke, K. West, L. N. Pfeiffer, A. G. Truscott, E. A. Ostrovskaya, J. Levinsen, and M. M. Parish, Bogoliubov excitations of a polariton condensate in dynamical equilibrium with an incoherent reservoir, Phys. Rev. B **105**, 224515 (2022).

[53] See Supplemental Material at http://link.aps.org/supplemental/10.1103/PhysRevB.109.085423 for detailed information on the microcavity sample, excitation scheme, experimental setup, and calculated MC transmission spectra.

[54] A. A. Demenev, D. D. Yaremkevich, A. V. Scherbakov, S. M. Kukhtaruk, S. S. Gavrilov, D. R. Yakovlev, V. D. Kulakovskii, and M. Bayer, Ultrafast strain-induced switching of a bistable cavity-polariton system, Phys. Rev. B **100**, 100301(R) (2019).

[55] A. A. Demenev, D. D. Yaremkevich, A. V. Scherbakov, S. S. Gavrilov, D. R. Yakovlev, V. D. Kulakovskii, and M. Bayer, Ultrafast all-optical polarization switch controlled by optically excited picosecond acoustic perturbation of exciton resonance in planar microcavities, Phys. Rev. Appl. **18**, 044045 (2022).

[56] A. S. Brichkin, S. I. Novikov, A. V. Larionov, and V. D. Kulakovskii, M. M. Glazov, C. Schneider, S. Höfling, M. Kamp, and A. Forchel, Effect of Coulomb interaction on exciton-polariton condensates in GaAs pillar microcavities, Phys. Rev. B **84**, 195301 (2011).

[57] Yu. M. Kagan, B. V. Svistunov, and G. V. Shlyapnikov, Kinetics of bose condensation in an interacting bose gas, Zh. Eksp. Teor. Fiz. **101**, 528 (1992).

[58] Yu. M. Kagan and B. V. Svistunov, Kinetics of the onset of long-range order during bose condensation in an interacting gas, Zh. Eksp. Teor. Fiz. **105**, 353 (1994).

[59] V. E. Hartwell and D. W. Snoke, Numerical simulations of the polariton kinetic energy distribution in GaAs quantum-well microcavity structures, Phys. Rev. B **82**, 075307 (2010).

[60] A. I. Tartakovskii, M. Emam-Ismail, R. M. Stevenson, M. S. Skolnick, V. N. Astratov, D. M. Whittaker, J. J. Baumberg, and J. S. Roberts, Relaxation bottleneck and its suppression in semiconductor microcavities, Phys. Rev. B **62**, R2283(R) (2000).

[61] A. A. Demenev, S. S. Gavrilov, and V. D. Kulakovskii, Stimulated parametric polariton-polariton scattering in GaAs microcavities with a shallow polariton band under resonant excitation of exciton mode, Phys. Rev. B **84**, 085305 (2011).